Journal of Applied Polymer Science

Experimental study of the rheological, mechanical, and dielectric properties of MgO/LDPE nanocomposites

Xiang Lin,[1] YunHui Wu,[1] Lu Yang Tang,[1] Min Hao Yang,[1] Dong Yun Ren,[2] Jun Wei Zha,[1] Zhi Min Dang[1]

[1]Department of Polymer Science and Engineering, School of Chemistry and Biological Engineering, University of Science and Technology Beijing, Beijing 100083, China

[2]College of Mechanical and Electrical Engineering, Beijing University of Chemical Technology, Beijing 100029, China

Correspondence to: Z. M. Dang (E-mail: dangzm@ustb.edu.cn)

ABSTRACT: The properties of the polymer nanocomposites (PNCs), consisting low density polyethylene (LDPE) and magnesium oxide nanoparticles (MgO-NPs), were systematically discussed in this paper. The shear mixing time and MgO concentration were considered as the two factors affecting the dispersion state, which was found to be effective to change the crystallinity and the mechanical performance of MgO/LDPE PNCs. A reduction in the dynamic shear viscosity was observed when the concentration of MgO-NPs at a relative low level, which was also dominant by the dispersion states of MgO-NPs. Evident enhancement of the static yield stress was revealed only by introducing a minute amount of MgO-NPs (0.25 wt %). Meanwhile, the elastic and loss modulus were also found to be dependent on the dispersion state of MgO-NPs. A positive increase in dielectric permittivity was identified by uniaxial stretching the MgO/LDPE PNCs strips owing to the orientation enhancement of internal microstructure. © 2015 Wiley Periodicals, Inc. J. Appl. Polym. Sci. **2016**, *133*, 43038.

KEYWORDS: composites; dielectric properties; viscosity and viscoelasticity

Received 26 June 2015; accepted 8 October 2015

DOI: 10.1002/app.43038

INTRODUCTION

Nanoparticles (NPs), usually inorganic, are favorably used as additives for improving mechanical,[1–3] thermal,[3,4] dielectric,[5,6] and other properties[7,8] of polymer matrix. Hypothetical network[4] and layer-by-layer[9,10] inner structures between the additive NPs and molecular chains are the most attractive mechanisms for explaining the reinforcement. The composites consisting magnesium oxide nanoparticles (MgO-NPs) and low density polyethylene (LDPE) has been found in various properties for electrical insulation of power cables. It was well documented that the introduction of nm-sized MgO particles can hinder the accumulation of space charge in the insulation, widely used in the high voltage DC cable.[11,12] However, the effects of MgO-NPs itself as well as its distribution state and concentration on the flow properties and the mechanical performance of LDPE matrix still lack a further insight.[13]

Scale effect,[14,15] dispersion efficiency,[16,17] and orientation degree[18] of the NPs are considered as the most important factors. Although introducing NPs can effectively improve the matrix's properties, on the other hand it generally leads to high viscosity and makes the processability disappointed. Viscous and elastic behaviors of PNCs were widely documented in many publications.[19–24] The particle–matrix interaction, melt surface tension, and complex entanglement were thought to be the dominant attributions to the viscosity increase. Viscosity reduction, however, was also reported in Jain's work[25] when a very small amount of silica-NPs were introduced into polypropylene matrix. NPs with higher aspect ratio and larger surface area as well as good compatibility with matrix resulted in higher interfacial strength and better mechanical performance, but higher melt viscosity was also revealed.[26–33]

The importance of interface layer was emphasized for the mechanical performance[3] and thermal stability of polymer composites,[4] which was largely determined by the distribution state. Thus, how to obtain a fine dispersion of NPs and how to functionalize the interfacial structure between NPs and matrix becomes very critical.[34,35] With a high interfacial interaction, significant solid-like behavior is exhibited for those PNCs with modified NPs than those with virgin NPs, even though the dispersion state of the modified NPs is poor.[36] For crystallized or semicrystallized polymers, the NPs are also found to be helpful

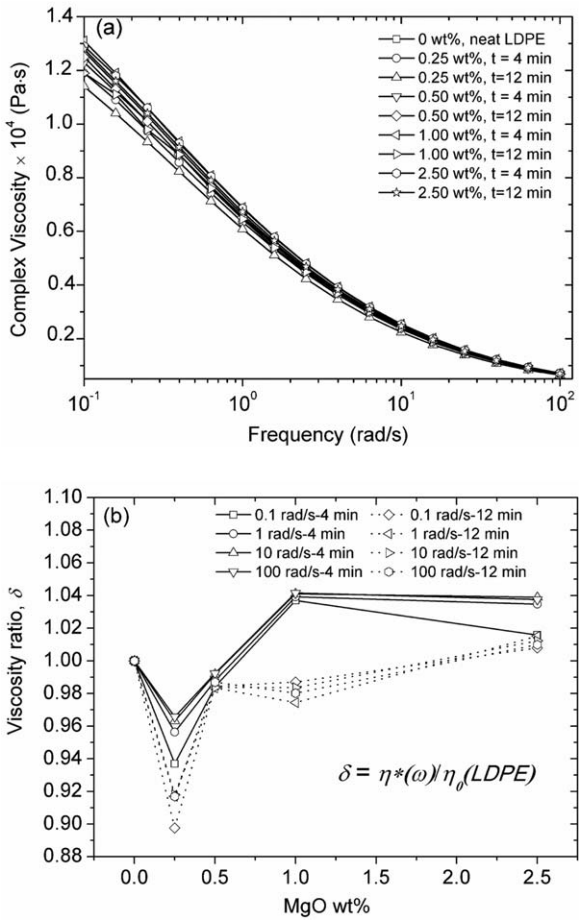

Figure 1. Dynamic shear viscosity (a) and viscosity ratio (b) of MgO/LDPE PNCs at 170°C.

to enhance the molecular chains orientation along the flow direction during extrusion, leading to an enhancement of mechanical performance.[37–40]

The present work is part of a larger project on developing MgO/LDPE nanocomposites for the application of high voltage DC power cables. Individually prepared MgO-NPs were employed for trapping the free ions or/and electrons and hindering the accumulation of space charge. The effects of concentration and distribution of MgO-NPs, shear mixing time, and orientation degree of molecular chains were taken into account as the factors affecting the intrinsic properties such as viscosity, kinetic crystallization, mechanical, and dielectric performances.

EXPERIMENTAL

Materials

Near spherical MgO-NPs with an average size of ca. 50 nm, a density of ca. 3.58 g/cm^3, and a dielectric permittivity of ca. 9.70 were adopted as the nanofiller. A series of weight contents as 0.25, 0.5, 1.0, 2.5, 5.0, 10, and 20 wt % were selected for preparing the MgO/LDPE PNCs. A LDPE (Sinopec) with a weight-average molecular weight ca. $M_w = 150$–160 kg mol^{-1} for the special application of high voltage DC power cable was used as the matrix.

Apparatus

Scanning Electron Microscopy (SEM). Surface morphological observations were conducted with Zeiss Supra 55 SEM at 20 kV. Conductive coating (using Pt) was done for the investigated surface and samples were prepared by breaking within liquid nitrogen (N_2). The detected surface should be fractured in liquid N_2 for protecting the natural morphology.

Rotational Rheometer. Rheological properties of the neat LDPE and the MgO/LDPE PNCs were measured by an advanced rheometer (Malvern Kinexus Ultra) under the oscillatory mode. Circular samples with a 2.0 mm thickness and a 25 mm diameter were hot molded under 120°C and 20 MPa. According to the "Cox–Merz equation", empirical relation between the dynamic viscosity $\eta^*(\omega)$, and the steady-shear viscosity $\eta(\dot{\gamma})$, usually is satisfactory, i.e., $\eta(\dot{\gamma})=\eta^*(\omega)$.

Dynamic Mechanical Thermal Analyzer (DMTA). Dynamic mechanical analyses were performed on a DMTA (TA Instrument Q800). Several rectangular strips with a thickness of 1.25 mm, a width of 3.0 mm, and a length of 30.0 mm were adopted for each measurement at the frequency of 1 Hz. The average data was taken as the final result for considering the G'/G''.

Differential Scanning Calorimeter (DSC). Calorimetric measurements were performed with SHIMADZU DSC-60 under a flowing nitrogen atmosphere. All the measurements were performed with a heating/cooling rate of 10°C min^{-1} from the room temperature to 150°C or vice versa. The crystallinity can be simply estimated by the DSC measurement based on eq. (1).

$$X_c = \frac{\Delta H}{\Delta H_0(1-\omega)} \times 100\%, \quad (1)$$

where X_c is crystallinity, ΔH is the measured enthalpy, and the ΔH_0 is the enthalpy with a 100% crystallization morphology, ω is the weight content of the MgO nanofillers.

Tensile apparatus. Measurements of tensile properties were carried out using a tensile device (JJ-Test) with a constant crosshead speed of 20 mm min^{-1} at room temperature. Five selected samples were employed and on the estimation of yield stress and elongation the averaged value was used.

Impedance Analyzer (IA). Dielectric properties of MgO/LDPE PNCs were measured using an IA system (Agilent 4294A). Samples, onto which silver electrodes had been painted, were tested under room temperature. Typical AC applied voltage was 1 V and the frequency ranges from 10^2 to 10^7 Hz. By means of this impedance analyzer, the dielectric constant can be calculated by

$$\varepsilon = \frac{C_p d}{\varepsilon_0 s}, \quad (2)$$

where ε is the permittivity of adopted sample, C_p is the measured capacitance, d is sample thickness, s is surface area of coated electrode, and ε_0 is the permittivity of free space with a constant ca. 8.854×10^{-12} F m^{-1}.

X-ray Diffractometer (XRD). The crystallization morphology was detected with an XRD (Rigaku D_{MAX}-RB 12 kW) using a

Cu-Kα radiation source ($\lambda = 1.5406$ Å). The measured angle ranged from 5° to 50° with a step width of 0.02°.

Preparation of Specimens

Although a better NPs dispersion state was obtained by solution mixing at low concentration than melt compounding, reversed result was reported when additive concentration was up to 5.0 wt %.[41] Standing on the mass producing perspectives, however, the solution mixing is low productive. Here, therefore, MgO/LDPE PNCs were prepared by melt blending through a batch mixer (Haake Polylab QC). For studying the effect of shear mixing time on the dispersion state of NPs, rotor speed was chosen at 60 rpm for duration times of 4 and 10 min, respectively. Specimens for all the measurements were hot compressed at 120°C.

RESULTS AND DISCUSSIONS

3.1Viscosity Dependence on the MgO-NPs Concentration

Viscosity, representing the flow ability of a viscous liquid, was emphasized for the rheological study of MgO/LDPE PNCs melts. In common sense, the immiscibility between the matrix and the nano-inclusions usually causes the so-called rheological degradation, i.e., dramatically increasing the viscosity.[11,16,24,26] For seeking the viscosity percolation threshold, special attention was given to those MgO/LDPE PNCs with low amount of MgO-NPs. All the measurements were conducted with a shear strain amplitude of 1% and a constant temperature of 170°C, as shown in Figure 1(a). In order to exclude the influence of molecular degradation, the neat LDPE was also applied the same shear history, i.e., melting and "mixing" under the same process conditions.

The complex shear viscosity of the MgO/LDPE PNCs divided by the one of neat LDPE measured at the same frequency is defined as the viscosity ratio δ, as given in Figure 1(b). Apart from the typical shear thinning which is shown from the plots of viscosity η versus frequency ω, a viscosity reduction is further observed for those MgO/LDPE PNCs melts with a low amount of MgO-NPs. For instance, viscosity reduction of the samples mixed for 4 min can be observed up to the MgO-NPs loading of 0.5 wt %, while for the samples mixed for 12 min this reduction can be still found up to 1.0 wt %.

The decrease of the viscosity at low MgO-NPs concentration could be attributed to the increase of free volume between the LDPE chains and the MgO-NPs, i.e., the interface effect. Jain *et al.*[25] had emphasized the importance of free volume and interaction bridges between nanofiller and molecular chains, based on which the viscosity varies significantly. The increase of free volume decreases dramatically the internal friction resistance among the molecular chains during the PNCs melts flowing, leading to apparent decrease of viscosity. Similar mechanism was also mentioned by Merkel *et al.*[42] However, Merkel pointed out that this was largely dependent on the size and the aggregation degree of NPs. Part of the polymer chains and/or segments could selectively adsorb to the NPs surface owing to the Van der Waals' force, developing a similar "cross-link" structure. When the NPs concentration exceeds the percolation threshold, it is supposed that the dispersed inclusions

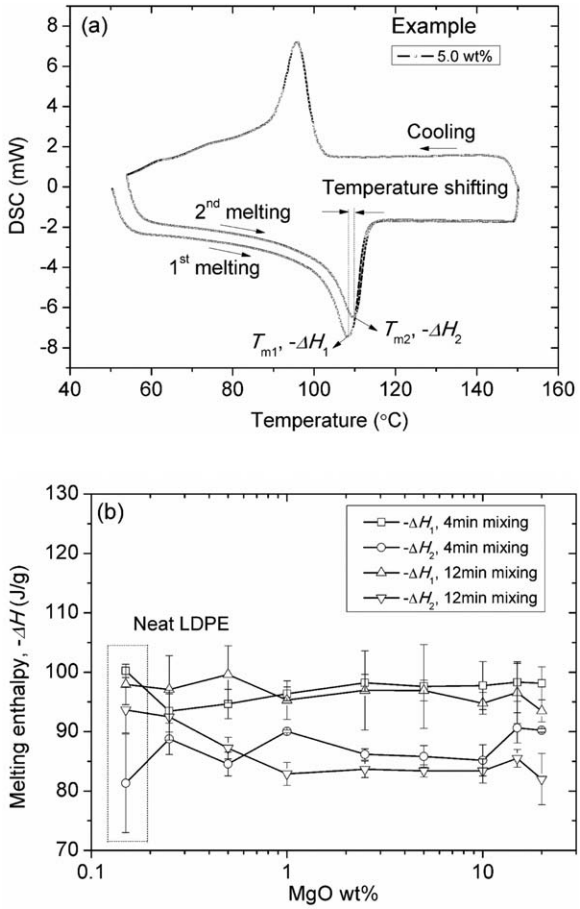

Figure 2. Running process of the DSC testing (a) and comparison of the melting enthalpy ΔH (b).

acted the role of knitting points and could promote the local entanglement degree of molecular chains, which is dependent on the specific area of the dispersed particles and clusters. It can be imagined that if the nanoadditives were dispersed individually well enough within the viscoelastic matrix, the nanocomposite melt could be show the dilatants fluid behavior but not pseudoplastic anymore. Therefore, for the immiscible compounding system, the different mixing time could lead to different dispersion states of the NPs, causing a different variation of the free volume.

Kinetics of Crystallization Behavior

A better understanding of the effect of mixing time on crystallization kinetics can be obtained by DSC measurement, as shown in Figure 2(a). The MgO/LDPE PNCs with 5.0 wt % MgO-NPs was selected as an example for discussion. The first melting process aims to explore the shear mixing time effect and the second melting is going to further study the effects of concentration and dispersion state. The onset and the endset temperatures for analyzing ΔH were selected at 101–103 and 112–114°C, respectively.

It can be found that during the second melting process the melting temperatures T_m of all the MgO/LDPE PNCs as well as the neat LDPE were almost equally appeared at 109.6 ± 0.3°C.

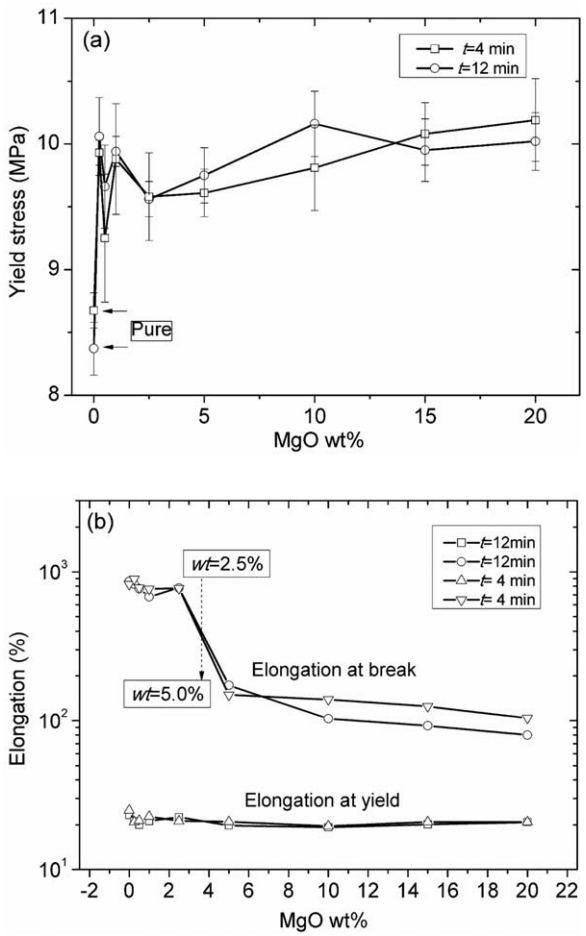

Figure 3. Effect of weight content of MgO on the yield strength (a) and elongation (b).

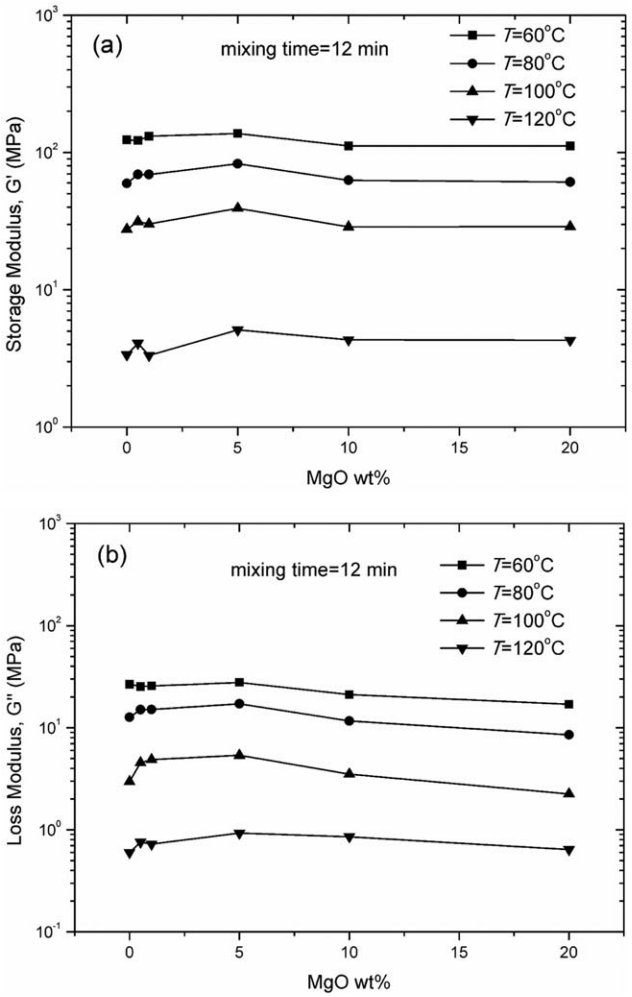

Figure 5. Dependence of G' (a) and G'' (b) of MgO/LDPE PNCs on the loading of MgO-NPs.

This indicates that the kinetic crystallization behavior of the MgO/LDPE PNCs is mainly determined by the intrinsic properties of LDPE matrix. Figure 2(b) further reveals that the MgO-NPs concentration plays a noneffective role on the melting enthalpy ΔH, i.e., the crystallinity of LDPE cannot be significantly changed just by incorporating with MgO. However, an effective dispersion of NPs is confirmed to be helpful to enhance crystallinity. Benefited from the shear mixing, enhanced enthalpy is revealed from the $\Delta H_1 > \Delta H_2$. The applied shear is helpful to increase the local orientation degree of molecular chains and to improve the crystallinity, but this is not absolute in case of degradation of molecular chains.

Mechanical Properties

The relationship between the mechanical performance and the NPs concentration was discussed by tensile performance, as shown in Figure 3(a). Specimens for this measurements were

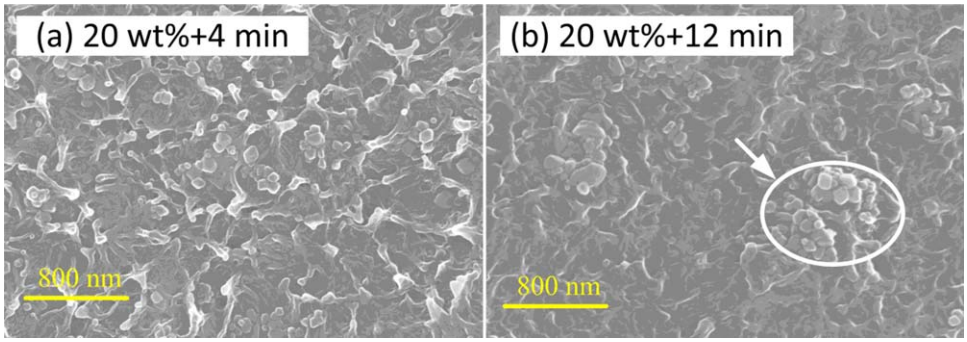

Figure 4. Effect of the mixing time on the dispersion state of MgO-NPs within matrix. [Color figure can be viewed in the online issue, which is available at wileyonlinelibrary.com.]

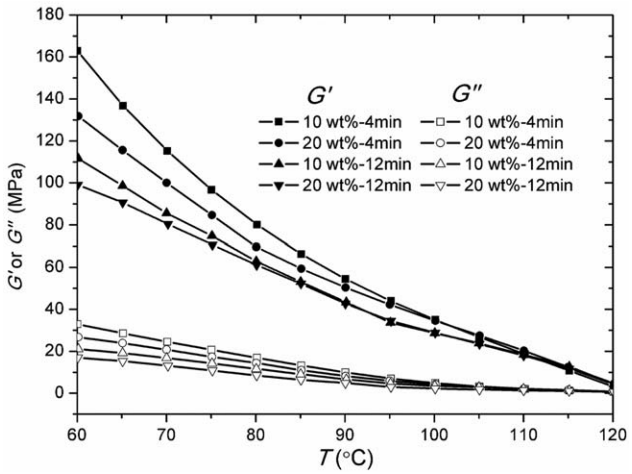

Figure 6. Effects of MgO-NPs concentration and shear time on G' (a) and G'' (b) of MgO/LDPE PNCs.

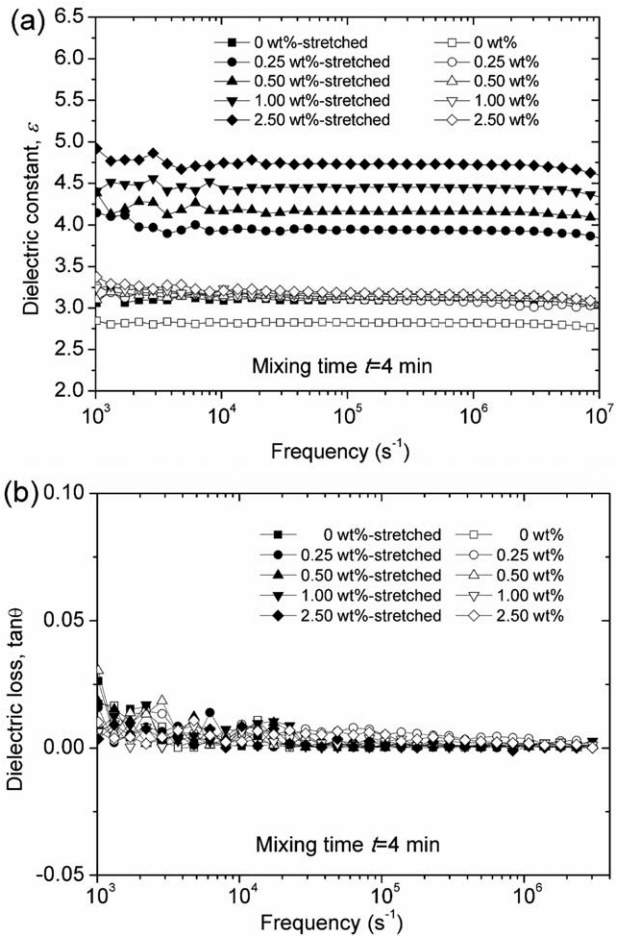

Figure 8. Dielectric properties: (a) dielectric constant; (b) dielectric loss. Samples adopted for this measurement were prepared under the mixing time of 4 min.

prepared with a geometrical dimension of 10 × 97 × 1.25 mm. It is found that a positive enhancement of yield strength can be obtained by introducing MgO-NPs. The measured yield stress increases with the content of introduced MgO-NPs. When the MgO content is above ca. 13 wt %, yield stress of the samples prepared under 4 min is higher than that prepared under 12 min. Comparing with the neat sample, a sharp increase of yield stress is achieved even at a low amount of MgO-NPs. The yield strength at 0.25 wt % increases by ca. 14.5% (4 min) and ca. 20.2% (12 min), respectively. It is identified that this increase is largely induced by the strengthening effect of NPs, which confines the mobility of molecular chains or segments. Yang *et al.*[43] also suggested that the mechanical enhancement of rigid NPs was significantly dependent on the volume of constraint polymer chains surrounding the NPs. In common sense, agglomerated particles passed by a long shear mixing time are much more probably dispersed in the highly viscous polymer melt than that with a short shear mixing time. When the mixing time comes to 12 min, however, high NPs content is negative to improve the yield strength any more. A better NPs dispersion state can be achieved at a lower concentration and a longer mixing time. The agglomeration at higher NPs concentration becomes more serious.

Tensile breakage is supposed to be dependent on either breakage of the molecular chains or desorption between chains and particles. Almost all the samples present a yield elongation value ca. 20 ± 5%, as shown in Figure 3(b). The break elongation further indicates a definite percolation behavior at ca. 2.5–5.0 wt % MgO-NPs, where there is a sharp decrease of elongation. The yield behavior is just a viscoelastic deformation which is related to the extendable stretch and unrecoverable slip of segments and main chains. With the increase of MgO-NPs, therefore, the possibility of internal defect, such as dispersion as well as

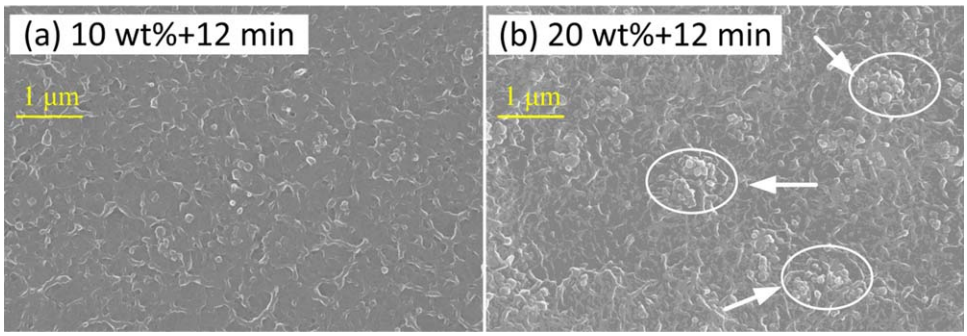

Figure 7. Comparison of the dispersion state of MgO/LDPE PNCs with 10 wt % and 20 wt % MgO-NPs under 12 min. [Color figure can be viewed in the online issue, which is available at wileyonlinelibrary.com.]

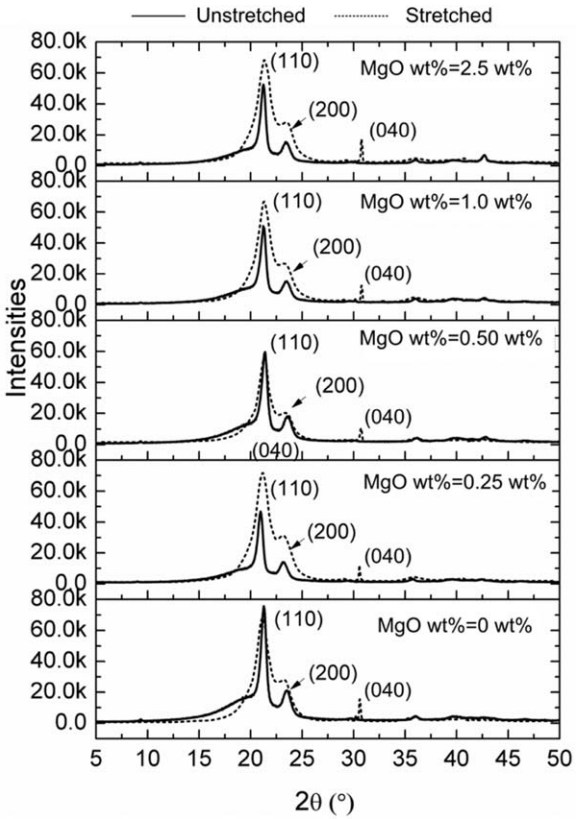

Figure 9. XRD patterns of MgO/LDPE PNCs corresponding to the samples in Figure 8.

interaction, will largely increase, leading to that above ca. 2.5 wt % MgO-NPs the elongation at break greatly decreases.

Generally, the breakage of NPs aggregation is helpful to increase the yield strength which can be estimated by static mechanical analysis. Uneven dispersion usually causes internal defects during continuous melt mixing, but this does not mean that the dispersion state is absolutely dependent on the mixing time.[44] The immiscibility between the matrix and nanoparticles could strongly promote the particles aggregation under a long mixing time. Constant shear mixing increases the possibility of one particle coming into contacting with another. With the help of the stronger interaction among particles, one particle adhering to the melt could be peeled off and then aggregation happens. When it comes to a nanocomposite with good compatibility, however, this situation could be inversed. In this work, a better dispersion state is obtained under 4 min when 20 wt % MgO-NPs were included, as shown in Figure 4.

Storage modulus G', representing the stiffness of an elastic isotropic material, and loss modulus G'', representing the dissipative property of a viscous isotropic material during the transformation between deformation and heat, were considered by dynamic mechanical analysis, as shown in Figure 5. Both G' and G'' are found to decrease slightly with the elevated temperatures. Under a certain temperature, a maximum G' and G'' is revealed for the samples with an additive amount of 5.0 wt %. Here, the dispersion state of MgO-NPs is positively affecting the modulus. Above 5.0 wt %, the tensile performance could be partly destroyed by particle aggregation clusters and then the viscoelastic property decreases. Below 5.0 wt %, however, the particles can be relatively dispersed well and then part of NPs play the role of temporary entangled knots, increasing the entanglement degree and restricting the segmental mobility of LDPE chains.[45,46] A comparison of the effect of mixing time on the dynamic properties is further shown in Figure 6. It is found that modulus (G' and G'') of MgO/LDPE PNCs with 10 wt % MgO-NPs is higher than those containing 20 wt %. This is also caused by the more significant aggregations of MgO-NPs under 12 min (comparing with 4 min) and the more interfacial defects under 20 wt % MgO-NPs (comparing with 10 wt %), which can be confirmed from the SEM observations, as shown in Figure 7.

Dielectric Property: The Orientation Effect

For a two-phase composite, its effective dielectric permittivity can be simply estimated by the rules of the mixture:[47]

$$\varepsilon_c = v_f \varepsilon_f + v_m \varepsilon_m, \quad (3)$$

where ε_c, ε_f, and ε_m are the permittivity of the composite, fillers, and the matrix, respectively. And v_f and v_m are the volume fractions of the fillers and the matrix, respectively. The higher the permittivity and/or volume fraction of fillers, the higher permittivity of composite will be obtained. It should be noted that the principle given in eq. (3) only can be used when the v_f is below the percolation threshold (v_c).

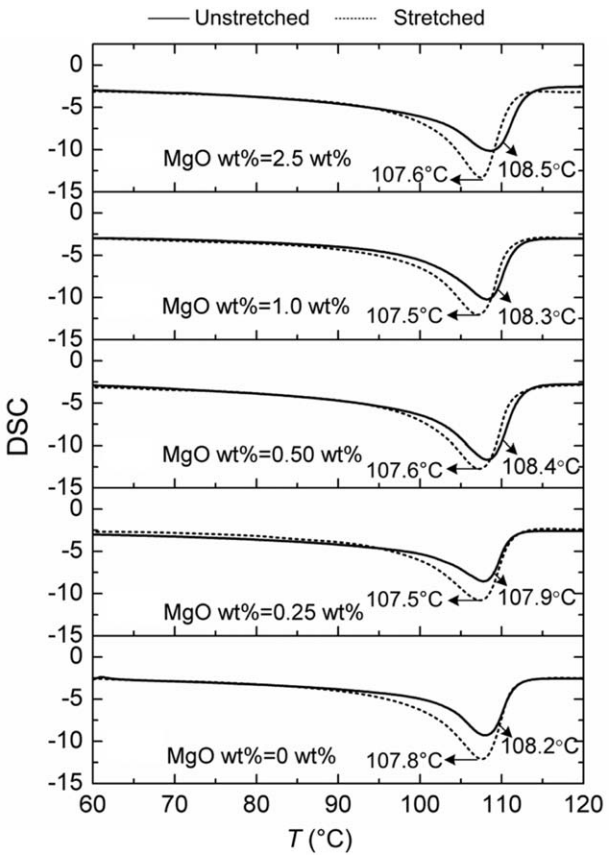

Figure 10. DSC melting peaks of the oral and the stretched MgO/LDPE PNCs samples.

Table I. Peak Melting Temperatures T, T_s, and Melting Enthalpies ΔH, ΔH_s of the MgO/LDPE PNCs from DSC Measurements

MgO (wt %)	0	0.25	0.50	1.0	2.5
T (peak) (°C)	108.0	107.7	108.2	108.2	108.6
T_s (peak) (°C)	107.6	107.3	107.3	107.1	107.2
ΔH (J g^{-1})	83.71	92.33	97.83	99.34	88.07
ΔH_s (J g^{-1})	107.25	113.55	114.41	114.14	111.08
δ (%)	28.12	22.98	16.95	14.90	25.92

T (peak) and T_s (peak) are the peak temperatures of the original and stretched samples, respectively. ΔH and ΔH_s are the melting enthalpies of the original and stretched samples, respectively. δ is the percentage increase of the melting enthalpy after stretching.

The effects of the MgO concentration and the orientation degree of molecular chains on dielectric permittivity were studied in this work, as shown in Figure 8. Stretched samples were prepared with a stretching ratio ca. 600% at room temperature. Compared with the neat LDPE ($\varepsilon = 2.75$), permittivity of the stretched neat LDPE reveals a slight increase (ca. 18%). For the stretched MgO/LDPE PNCs, a more significant enhancement is obtained, especially for the composite with 2.50 wt % MgO. The applied extension force is positive to reduce the aggregation clusters of MgO-NPs, subsequently achieving a better dispersion state after stretching. The dielectric loss shows almost no dependence on the MgO-NPs concentration or extensional effect, as shown in Figure 8(b). This provides a good potential for the energy storage application.

X-ray diffraction measurement was conducted for understanding the crystal microstructure. Three crystalline peaks for the stretched samples are presented in the XRD patterns, including the most general one at $2\theta = 20.9°$–$21.5°$ (110), the second one at 23.0°–23.6° (200), and the unique one at 36° (040), as shown in Figure 9. The increase in the intensity of the peaks of stretched samples indicates an increase in the crystalline nature.

The DSC measurements were further performed on the stretched samples, as shown in Figure 10. An obvious increase of the crystallinity (ca. 15–28%) and a decrease of the melting temperature are revealed, as seen in Table I. Melting temperature of unstretched samples increases slightly with the filler content; however, this phenomenon disappears after stretching the specimens and their melting temperatures hold at ca. 107.3 ± 0.3°C. This is because some well dispersed MgO-NPs substantially act as the role of crystal nucleus and induce the formation of spherical morphology. When the stretched deformation up to 600%, the regular arranged lamellae could be damaged, changing to similar fibrous morphology which presents a relatively low melting temperature. In addition, percentage increase of melting enthalpy δ is found to decrease with increasing the content of MgO-NPs up to 1.0 wt % while increasing again at 2.0 wt %, for which the aggregation of MgO-NPs should be responsible. A better distribution state of MgO-NPs could be achieved under a lower concentration. The big clusters will act the role of steric hindrance in the molecular thermal motion. Comparing with the pure LDPE, the crystal cells with a solid particle nuclei show a good resistance to the extension deformation, keeping the original crystallization morphology, hindering the growing of new crystal and finally decreasing the crystallinity of the stretched samples.

It is sure that the uniaxial extension is helpful to enhance the orientation of macromolecules and crystallites along the force direction, causing an increase of the interplanar crystal spacing. Some α-crystal cells are highly orientated, transforming to ellipsoid-shape crystal and inducing β crystallization phase (040) which presents higher dielectric permittivity than that of α phase. The unique peak revealed at the angular of ca. 30.25°–30.75° from the XRD patterns indicates this new phase. In addition, mechanical energy is continually converted to the internal energy of molecules during the stretching process, partially inducing the amorphous microcrystal morphology into the monoclinic phase and then directly increases the crystallinity.

CONCLUSIONS

Viscosity, kinetic crystallization, mechanical performance and dielectricity of MgO/LDPE PNCs were mainly studied in this paper. Owing to the increase of free volume, conspicuous percolation behavior was observed in the viscosity measurements just by introducing a low amount of MgO-NPs. Analysis of static mechanical properties showed that increasing the content of MgO-NPs and lengthening the mixing time were helpful to enhance the static yield strength. The dispersion state of MgO-NPs in the LDPE matrix was emphasized for this enhancement. For dynamic mechanical properties, similarly, a critical value of MgO-NPs concentration about 5.0 wt % was also observed. The storage modulus G' and loss modulus G'' increased with the increase of weight content below 5.0 wt %, but decreased with the increase of weight content above 5.0 wt %. As to the dielectric property, effective enhancement was considered at low concentration up to 2.5%. A new crystallization phase (040) was presented in the stretched samples suggested that an effective way to increase the dielectricity by drawing the MgO/LDPE PNCs at room temperature, which was largely attributed to the enhancement of orientation.

ACKNOWLEDGMENTS

The authors wish to thank the financial support of Beijing Natural Science Foundation (2142023), China Postdoctoral Science Foundation (2015M570928), National Natural Science Foundation of China (NSFC51473018, 51425201), State Key Laboratory of Electrical Insulation and Power Equipments (EIPE14204),

the Fundamental Research Funds for the Central Universities (FRF-TP-14-013A1).

REFERENCES

1. Xiao, K. Q.; Zhang, L. C.; Zarudi, I. *Compos. Sci. Technol.* **2007**, *67*, 177.
2. Jin, S. H.; Park, Y. B.; Yoon, K. H. *Compos. Sci. Technol.* **2007**, *67*, 3434.
3. Shokrollahi, P.; Mehmanchi, M.; Atai, M.; Omidian, H.; Shokrolahi, F. *J. Mater. Sci.***2014**, *25*, 23.
4. Bansal, M.; Yang, H.; Li, C.; Cho, K.; Benicewicz, B. C.; Kumar, S. K.; Schadler, L. S. *Nat. Mater.* **2005**, *4*, 693.
5. Fan, B. H.; Zha, J. W.; Wang, D. R.; Zhao, J.; Dang, Z. M. *Appl. Phys. Lett.* **2012**, *100*, 012903.
6. Wang, D. R.; Bao, Y. R.; Zha, J. W.; Dang, Z. M.; Hu, G. H. *ACS Appl. Mater. Interface* **2012**, *4*, 6273.
7. Byrne, M. T.; Gun'ko, Y. K. *Adv. Mater.* **2010**, *22*, 1672.
8. Jakubinek, M. B.; Ashrafi, B.; Zhang, Y. F.; Martinez-Rubi, Y.; Kingston, C. T.; Johnston, A.; Simard, B. *Compos. B: Eng.* **2014**, *69*, 87.
9. Wagner, H. D. *Nat. Nanotechnol.* **2007**, *2*, 742.
10. Podsiadlo, P.; Kaushik, A. K.; Arruda, E. M.; Waas, A. M.; Shim, B. S.; Xu, J. D.; Nandivada, H.; Pumplin, B. G.; Lahann, J.; Ramamoorthy, A.; Kotov, N. A. *Science* **2007**, *318*, 80.
11. Zhang, L.; Zhou, Y. X.; Tian, J. H.; Sha, Y. C.; Zhang, Y. X.; Wu, H. Z.; Wang, Y. S. *J. Electrostat.* **2014**, *72*, 252.
12. Takada, T.; Hayase, Y.; Tanaka, Y.; Okamoto, T. *IEEE Trans. Dielectr. Electr. Insul.* **2008**, *15*, 152.
13. Zhao, H.; Peng, S. Y.; Yang, J. M. *Adv. Mater. Res.* **2014**, *833*, 339.
14. Wan, T.; Liao, S.; Wang, K. P.; Yan, P.; Clifford, M. *Compos. A: Appl. Sci.* **2013**, *50*, 31.
15. Cai, D. Y.; Song, M. *Carbon* **2008**, *46*, 2107.
16. Irene, H.; Thomas, B. *J. Appl. Polym. Sci.* **2013**, *128*, 2098.
17. Tran, T. A.; Said, S.; Grohen, Y. *Compos. A: Appl. Sci.* **2005**, *36*, 461.
18. Kiziltas, A.; Nazari, B.; Gardner, D. J.; Bousfield, D. W. *Polym. Eng. Sci.* **2013**, *54*, 739.
19. Gupta, A.; Choudhary, V. *J. Mater. Sci.* **2014**, *49*, 3839.
20. Jancar, J.; Douglas, J. F.; Starr, F. W.; Kumar, S. K.; Cassagnau, P.; Lesser, A. J.; Sternstein, S. S.; Buehler, M. J. *Polymer* **2010**, *51*, 3321.
21. Sulong, A. B.; Ramli, M. I.; Hau, S. L.; Sahari, J.; Muhamad, N.; Suherman, H. *Compos. B: Eng.* **2013**, *50*, 54.
22. Yang, Z.; Cao, B.; Zhu, J. M.; Shen, J. B.; Li, J.; Guo, S. Y.; Wang, Y. Z. *Polym. Compos.* **2012**, *33*, 1432.
23. Hui, S.; Chaki, T. K.; Chattopadhyay, S. *Polym. Compos.* **2010**, *31*, 377.
24. Kharchenko, S. B.; Douglas, J. F.; Obrzut, J.; Grulka, E. A.; Migler, K. B. *Nat. Mater.* **2004**, *3*, 564.
25. Jain, S.; Goossens, J. P.; Peters, G. M.; van Duin, M.; Lamstra, P. *Soft Matter* **2008**, *4*, 1848.
26. Anand, A.; Harshe, R.; Joshi, M. *J. Appl. Polym. Sci.* **2013**, *129*, 1618.
27. Stankovich, S.; Dikin, D. A.; Dommett, G. B.; Kohlhaas, K. M.; Zimner, E. J.; Stach, E. A.; Piner, R. D.; Nguyen, S. T.; Ruoff, R. S. *Nature* **2006**, *442*, 282.
28. Sabzi, M.; Jiang, L.; Atai, M.; Ghasemi, I. *J. Appl. Polym. Sci.* **2013**, *129*, 1734.
29. Rafiee, M. A.; Rafiee, J.; Wang, Z.; Song, H. H.; Yu, Z. Z.; Koratkar, N. *ACS Nano* **2009**, *3*, 3884.
30. He, Z. P.; Zhang, X. H.; Chen, M. H.; Li, M.; Gu, Y. Z.; Zhang, Z. G.; Li, Q. W. *J. Appl. Polym. Sci.* **2013**, *129*, 3366.
31. Du, F.; Scogna, R. C.; Zhou, W.; Brand, S.; Fischer, J. E.; Winey, I. *Macromolecules* **2004**, *37*, 9048.
32. Huang, Y. Y.; Ahir, S. V.; Terentjev, E. M. *Phys. Rev. B* **2006**, *73*, 125422.
33. Hu, G. J.; Zhao, C. G.; Zhang, S. M.; Yang, M. S.; Wang, Z. G. *Polymer* **2006**, *47*, 480.
34. Chen, D.; Wang, M.; Zhang, W. D.; Liu, T. X. *J. Appl. Polym. Sci.* **2009**, *113*, 644.
35. Sadasivuni, K. K.; Saiter, A.; Gautier, N.; Thomas, S.; Grohens, Y. *Colloid. Polym. Sci.* **2013**, *291*, 1729.
36. Wen, R.; Ke, K.; Wang, Y.; Yang, W.; Xie, B. H.; Yang, M. B. *J. Appl. Polym. Sci.* **2011**, *121*, 3041.
37. Wang, J. B.; Li, Y. G.; Weng, G. S.; Jiang, Z. Q.; Chen, P.; Wang, Z. B.; Gu, Q. *Compos. Sci. Technol.* **2014**, *96*, 63.
38. Ning, N. Y.; Fu, S. R.; Zhang, W.; Chen, F.; Wang, K.; Deng, H.; Zhang, Q.; Fu, Q. *Prog. Polym. Sci.* **2012**, *37*, 1425.
39. Moussaif, N.; Groeninckx, G. *Polymer* **2003**, *44*, 7899.
40. Chatterjee, A.; Mishra, S. J. *Polym. Res.* **2013**, *20*, 1.
41. Ke, K.; Wang, Y.; Liu, X. Q.; Cao, J.; Luo, Y.; Yang, W.; Xie, B. H.; Yang, M. B. *Compos. B: Eng.* **2012**, *43*, 1425.
42. Merkel, T. C.; Freeman, B. D.; Spontak, R. J.; He, Z.; Pinnau, I.; Meakin, P.; Hill, A. *Science* **2002**, *296*, 519.
43. Yang, J.; Zhao, J. J.; Xu, F.; Sun, R. C. *ACS Appl. Mater. Interface* **2013**, *5*, 12960.
44. Li, J.; Ma, P. C.; Chow, W. S.; To, C. K.; Tang, B. Z.; Kim, J. K. *Adv. Funct. Mater.* **2007**, *17*, 3207.
45. Saha, A. K.; Das, S.; Bhatta, D.; Mitra, B. C. *J. Appl. Polym. Sci.* **1999**, *71*, 1505.
46. Jayanarayanan, K.; Thomas, A.; Joseph, K. *Compos. A: Appl. Sci.* **2008**, *39*, 164.
47. Hossain, M. E.; Liu, S. Y.; O'Brien, S.; Li, J. *Acta Mech.* **2014**, *225*, 1197.